Journal of Sound and Vibration (1997) **204**(1), 131–158

VIBRATIONS OF OPEN-SECTION CHANNELS: A COUPLED FLEXURAL AND TORSIONAL WAVE ANALYSIS

Y. YAMAN

Department of Aeronautical Engineering, *Middle East Technical University*, 06531 *Ankara*, *Turkey*

(*Received* 22 *July* 1996, *and in final form* 30 *January* 1997)

An exact analytical method is presented for the analysis of forced vibrations of uniform, open-section channels. The centroid and the shear center of the channel cross-sections considered do not coincide; hence the flexural and the torsional vibrations are coupled. In the context of this study, the type of any existing coupling is defined in terms of the independent motions which are coupled through mass and/or stiffness terms. Hence, if the flexural vibrations in one direction are coupled with the torsional vibrations, the resulting coupling is called double-coupling. On the other hand, if the flexural vibrations in two mutually perpendicular directions and the torsional vibrations are all coupled, the resulting coupling is referred to as triple-coupling. The study also takes the effects of cross-sectional warping into consideration but, since it is derived from torsional characteristics, the warping is not treated as an independent motion. Wherever necessary, the admission of warping is characterized by the inclusion of warping constraint. The current work uses the wave propagation approach in constructing the analytical model. Single-point force excitation has been considered throughout and the channels are assumed to be of Euler–Bernoulli beam type. Both double- and triple-coupling analyses are performed. The coupled wavenumbers, various frequency response curves and the mode shapes are presented for undamped and structurally damped channels.

1. INTRODUCTION

Open-section channels are widely used in aeronautical structures as stiffeners. In general, they have a cross-section in which the centroid and the shear centre do not coincide. This leads to the phenomenon that the flexural vibrations are coupled with the torsional vibrations.

This complicated problem has attracted scientists for a long time. One of the early analytical works in this field was performed by Gere *et al*. [1]. They determined the coupled, free vibration characteristics of uniform, open-section channels using the Rayleigh–Ritz method. Later Lin [2], again by using the same energy method, analyzed the triply coupled free vibration characteristics of a skin–stringer configuration. In reference [3], Bishop *et al*. compared the effectivenesses of various beam theories in the solution of beams having coupled torsion and bending. Dokumacı [4] developed an exact analytical model for the determination of coupled vibration characteristics of open-section channels which were symmetric with respect to an axis. The warping was not admitted. In reference [5], Bishop *et al*. allowed the cross-sectional warping in Dokumacı's theory and investigated the doubly coupled Euler–Bernoulli beams of open cross-section. All of

0022–460X/97/260131 + 28 $25.00/0/sv970933

these works, although pioneering in nature, fell short of providing an answer to the forced vibration characteristics and included only the classical end boundary conditions.

Cremer and Heckl [6] proposed a method for analyzing the forced wave motion in uniform structures. The use of that method was found to be extremely useful when the responses of uniform structures to point harmonic forces or line harmonic loads were calculated. Mead and Yaman then presented analytical models for the analysis of forced vibrations of Euler–Bernoulli beams [7, 8]. In reference [7], they considered finite length beams, both periodic and non-periodic, and studied the effects of various classical or non-classical boundary conditions on the flexural response. In reference [8] attention was focused on infinite and periodic beams. One of the bays was subjected to a point harmonic force. Effects of support characteristics, excitation and response locations were fully dealt with.

What follows here is a study of the forced, coupled vibration characteristics of uniform cross-section channels. The channel cross-sections are either symmetric with respect to an axis or there exists no axial symmetry. Consequently, either only the flexural vibrations in one direction are coupled with the torsional vibrations (doubly coupled case) or both flexural vibrations and the torsional vibrations do simultaneously occur (triply coupled case). The mathematical model for the analysis of coupled vibrations is being formulated by using the wave propagation approach [6, 7]. The forcing is taken in the form of a point harmonic load. The end conditions are assumed to be classical and hence simply supported, clamped and free ends are taken into consideration.

The effects of the cross-sectional warping constraint are fully dealt with. Both damped and undamped analyses are performed. The method developed, although basically aimed at the determination of forced vibration characteristics, is also capable of finding free vibration properties. This is also illustrated, by plotting the various mode shapes.

2. THEORY

2.1. WAVE PROPAGATION IN UNIFORM EULER–BERNOULLI BEAMS

It is known that the total forced response of a linear, uniform, finite beam is a superposition of the forced response of the beam as if it were infinite and the free response of the beam as if it were finite. Hence, in this study the beam responses are determined as the sum of the response of an infinite beam to a point load together with the waves reflected from the ends of the finite beam.

In Figure 1 represented an infinite and a finite Euler–Bernoulli beam, each of which is subjected to a point, harmonically varying force. The generated and reflected waves (if any) for each case are also shown. Consider Figure 1(a), which shows a uniform, infinite Euler–Bernoulli beam on which a point harmonic force $F_0\,e^{i\omega t}$ acts at $x = 0$. As can be seen,

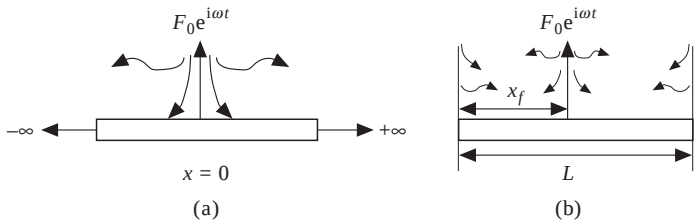

Figure 1. A uniform Euler–Bernoulli beam subjected to a point harmonic force. (a) Infinite beam, generated waves; (b) finite beam, generated waves and the waves reflected from the ends.

the application of the force creates a pair of waves which travel away from the point of excitation in each direction. In the absence of damping one of the two waves, travelling in either direction, has a purely real wave number defining a non-propagating wave and the other one has a purely imaginary wave number representing a propagating wave. These waves are called the *forced waves* and the total transverse displacement of the infinite beam at any $|x|$ can be found to be [6]

$$w(x, t) = F_0 \sum_{n=1}^{N} a_n \, e^{-k_n |x|} \, e^{i\omega t}. \tag{1}$$

N defines the so-called degree-of-freedom of the structure cross-section and for an Euler–Bernoulli beam $N = 2$, the degrees of freedom being the transverse displacement w and the slope dw/dx. k_n is the nth wavenumber of the beam ($k_n = (m\omega^2/EI)^{1/4}$). The a_n values are the complex wave component amplitudes which are to be found by satisfying the relevant compatibility and continuity conditions at the point of application of the point harmonic force [7]. (A list of nomenclature is given in Appendix B.)

Now consider Figure 1(b). It represents a beam which is finite in length. Any forced waves generated by the external excitation $F_0 e^{i\omega t}$ acting at $x = x_f$ will be reflected from the ends of the beam. These reflected waves are called the *free waves*. In an Euler–Bernoulli beam there are four free waves and the transverse displacement due to them is given by

$$w(x, t) = \sum_{n=1}^{4} A_n \, e^{k_n x} \, e^{i\omega t}. \tag{2}$$

Hence, the total harmonic transverse displacement of the beam at any x ($0 < x < L$) can be found to be

$$w(x, t) = \left(\sum_{n=1}^{4} A_n \, e^{k_n x} + F_0 \sum_{n=1}^{2} a_n \, e^{-k_n |x - x_f|} \right) e^{i\omega t}. \tag{3}$$

The A_n values are the complex amplitudes of the free waves and are found by satisfying the relevant boundary conditions at the ends of the beam. Once determined, their substitution into equation (3) yields the transverse displacement at any point of the finite beam. More comprehensive information can be found in reference [7].

2.2. DOUBLY COUPLED VIBRATIONS

Consider Figure 2, in which is shown a typical open cross-section, which is symmetric with respect to the y-axis. A transverse force applied through the centroid C results in a transverse force through the shear centre O and a twisting torque about O. The real and the effective loadings are illustrated in Figure 2(b).

In this case the flexural vibrations in the z direction are coupled with the torsional vibrations whereas the flexural vibrations in the y direction occur independently. The equations of motion for these types of coupled vibrations are known to be [1, 2]

$$EI_\xi \frac{\partial^4 w}{\partial x^4} + m \frac{\partial^2 w}{\partial t^2} + mc_y \frac{\partial^2 \phi}{\partial t^2} = 0, \qquad E\Gamma_0 \frac{\partial^4 \phi}{\partial x^4} - GJ \frac{\partial^2 \phi}{\partial x^2} + mc_y \frac{\partial^2 w}{\partial t^2} + \rho I_0 \frac{\partial^2 \phi}{\partial t^2} = 0, \tag{4}$$

where w is the flexural displacement in the z direction, ϕ is the torsional displacement, EI_ξ is the flexural rigidity in the z direction, GJ is the torsional stiffness, m is the mass per unit length, c_y is the eccentricity between the centroid and the shear centre in the y direction,

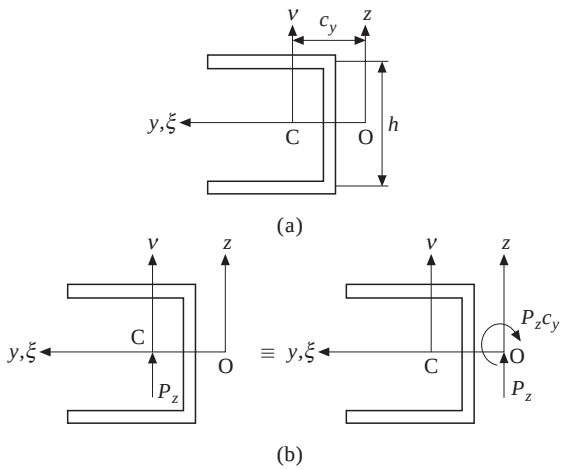

Figure 2. A typical cross-section of double-coupling. (a) Co-ordinate system; (b) real and effective loadings.

ρ is the material density, I_0 is the second polar moment of area with respect to the shear centre, and $E\Gamma_0$ is the warping stiffness with respect to the shear centre.

If one assumes that

$$w(x, t) = w_n \, e^{k_n x} \, e^{i\omega t}, \qquad \phi(x, t) = \phi_n \, e^{k_n x} \, e^{i\omega t}, \tag{5}$$

the expansion of equation (4), together with the expressions (5), gives the following equation for the wavenumbers:

$$(EI_\xi)\,(E\Gamma_0)k_n^8 - (EI_\xi)\,(GJ)k_n^6 - ((\rho I_0\,\omega^2)\,(EI_\xi) + (E\Gamma_0)\,(m\omega^2))k_n^4 + (GJ)\,(m\omega^2)k_n^2 + (\rho^2 A I_0 - c_y^2\,\rho^2 A^2)\omega^4 = 0. \tag{6}$$

Here A is the constant cross-sectional area and ω is the angular frequency. This equation is of eighth order and yields eight wavenumbers in four positive and negative pairs ($j = 4$). These waves are influenced by both the flexural and the torsional properties of the structure and describe the doubly coupled motion characteristics.

Note that the exclusion of warping constraint from the analysis reduces equation (6) to sixth order:

$$(EI_\xi)\,(GJ)k_n^6 + (\rho I_0\,\omega^2)\,(EI_\xi)k_n^4 - (GJ)\,(m\omega^2)k_n^2 - (\rho^2 A I_0 - c_y^2\,\rho^2 A^2)\omega^4 = 0. \tag{7}$$

Equation (7) now gives six wavenumbers in positive and negative pairs ($j = 3$).

Following the theory outlined in section 2.1, one can conclude that a force P_z through the centroid will create the following forced waves at any $|x|$ along the length of the channel:

$$w(x, t) = P_z \sum_{n=1}^{j} a_n \, e^{-k_n |x|} \, e^{i\omega t}, \qquad \phi(x, t) = P_z \sum_{n=1}^{j} c_n \, e^{-k_n |x|} \, e^{i\omega t}. \tag{8}$$

By using equations (4) and (5) the required c_n values can be found to be

$$c_n = \Psi_n \, a_n, \qquad \Psi_n = [(EI_\xi \, k_n^4 - m\omega^2)/(mc_y\,\omega^2)]. \tag{9}$$

The a_n values can be found by satisfying the following compatibility and continuity

conditions:

$$EI_\xi\, \partial^3 w(x,t)/\partial x^3\,|_{x=0} = P_z\,/2, \qquad \partial w(x,t)/\partial x\,|_{x=0} = 0,$$

$$T(x) = GJ\,\frac{\partial\phi(x,t)}{\partial x}\bigg|_{x=0} - E\Gamma_0\,\frac{\partial^3\phi(x,t)}{\partial x^3}\bigg|_{x=0} = \frac{P_z\,c_y}{2},$$

$$u(x,t) = -2A_s\,\frac{\partial\phi(x,t)}{\partial x}\bigg|_{x=0} = 0. \tag{10}$$

Here A_S is the swept area and $T(x)$ is the torque.

Equations (10), together with equations (8) and (9) can be cast into a fourth order matrix equation and the required a_n values found numerically.

Note that if the warping constraint is excluded from the analysis equations (10) become

$$EI_\xi\, \partial^3 w(x,t)/\partial x^3\,|_{x=0} = P_z\,/2, \qquad \partial w(x,t)/\partial x\,|_{x=0} = 0, \qquad GJ\,\partial\phi(x,t)/\partial x\,|_{x=0} = P_z\,c_y\,/2. \tag{11}$$

This simultaneously reduces the order of matrix equation for the a_n's to three.

Now, by including the effects of the $2j$ free waves as well, the total displacements can be found to be

$$w(x,t) = \left(\sum_{n=1}^{2j} \mathrm{e}^{k_n x} A_n + P_z \sum_{n=1}^{j} a_n\,\mathrm{e}^{-k_n|x-x_f|}\right)\mathrm{e}^{\mathrm{i}\omega t},$$

$$\phi(x,t) = \left(\sum_{n=1}^{2j} \mathrm{e}^{k_n x}\Psi_n\,A_n + P_z \sum_{n=1}^{j} c_n\,\mathrm{e}^{-k_n|x-x_f|}\right)\mathrm{e}^{\mathrm{i}\omega t}. \tag{12}$$

If included in the analysis, the warping displacement can be found to be

$$u(x,t) = -2A_s\,\frac{\partial\phi(x,t)}{\partial x} = -2A_s\left(\sum_{n=1}^{2j} k_n\,\mathrm{e}^{k_n x}\Psi_n\,A_n - P_z \sum_{n=1}^{j} c_n\,k_n\,\mathrm{e}^{-k_n|x-x_f|}\right)\mathrm{e}^{\mathrm{i}\omega t}. \tag{13}$$

The A_n values are found by satisfying the necessary $2j$ end boundary conditions. For a variety of classical end conditions, the boundary conditions are known to be as follows:

simply supported ends,

$j = 3$, $\quad w(0) = w(L) = w''(0) = w''(L) = \phi(0) = \phi(L) = 0,$

$j = 4$, $\quad w(0) = w(L) = w''(0) = w''(L) = \phi(0) = \phi(L) = \phi''(0) = \phi''(L) = 0;$

clamped ends,

$j = 3$, $\quad w(0) = w(L) = w'(0) = w'(L) = \phi(0) = \phi(L) = 0,$

$j = 4$, $\quad w(0) = w(L) = w'(0) = w'(L) = \phi(0) = \phi(L) = \phi'(0) = \phi'(L) = 0;$

free ends,

$j = 3$, $\quad w''(0) = w''(L) = w'''(0) = w'''(L) = \phi'(0) = \phi'(L) = 0,$

$j = 4$, $\quad w''(0) = w''(L) = w'''(0) = w'''(L) = T(0) = T(L) = \phi''(0) = \phi''(L) = 0;$ (14)

Here, $' = \partial/\partial x$, $'' = \partial^2/\partial x^2$ and $''' = \partial^3/\partial x^3$.

When the expressions (12) (if warping constraint is included also in equation (13)) are substituted into the relevant equations (14), a matrix equation is obtained. For the case of simply supported ends, no warping constraint and a unit force P_z the following equations can be found:

$$w(0) = 0, \quad \left(\sum_{n=1}^{2j} A_n + \sum_{n=1}^{j} a_n \, \mathrm{e}^{-k_n |x_f|} \right) = 0,$$

$$w''(0) = 0, \quad \left(\sum_{n=1}^{2j} k_n^2 \, A_n + \sum_{n=1}^{j} k_n^2 \, a_n \, \mathrm{e}^{-k_n |x_f|} \right) = 0,$$

$$\phi(0) = 0, \left(\sum_{n=1}^{2j} \Psi_n \, A_n + \sum_{n=1}^{j} \Psi_n \, a_n \, \mathrm{e}^{-k_n |x_f|} \right) = 0,$$

$$\phi(L) = 0, \left(\sum_{n=1}^{2j} \Psi_n \, \mathrm{e}^{k_n L} A_n + \sum_{n=1}^{j} \Psi_n \, a_n \, \mathrm{e}^{-k_n |L - x_f|} \right) = 0,$$

$$w''(L) = 0, \left(\sum_{n=1}^{2j} k_n^2 \, \mathrm{e}^{k_n L} A_n + \sum_{n=1}^{j} k_n^2 \, a_n \, \mathrm{e}^{-k_n |L - x_f|} \right) = 0,$$

$$w(L) = 0, \left(\sum_{n=1}^{2j} \mathrm{e}^{k_n L} A_n + \sum_{n=1}^{j} a_n \, \mathrm{e}^{-k_n |L - x_f|} \right) = 0. \tag{15}$$

These equations can be cast into the following matrix form:

$$\begin{bmatrix} 1 & 1 & 1 & 1 & 1 & 1 \\ k_1^2 & k_1^2 & k_2^2 & k_2^2 & k_3^2 & k_3^2 \\ \Psi_1 & \Psi_1 & \Psi_2 & \Psi_2 & \Psi_3 & \Psi_3 \\ \Psi_1 e_1 & \Psi_1 e_{-1} & \Psi_2 e_2 & \Psi_2 e_{-2} & \Psi_3 e_3 & \Psi_3 e_{-3} \\ k_1^2 e_1 & k_1^2 e_{-1} & k_2^2 e_2 & k_2^2 e_{-2} & k_3^2 e_3 & k_3^2 e_{-3} \\ e_1 & e_{-1} & e_2 & e_{-2} & e_3 & e_{-3} \end{bmatrix} \begin{Bmatrix} A_1 \\ A_2 \\ A_3 \\ A_4 \\ A_5 \\ A_6 \end{Bmatrix} = - \begin{Bmatrix} \sum_{n=1}^{3} a_n \, \mathrm{e}^{-k_n x_f} \\ \sum_{n=1}^{3} k_n^2 \, a_n \, \mathrm{e}^{-k_n x_f} \\ \sum_{n=1}^{3} \Psi_n \, a_n \, \mathrm{e}^{-k_n x_f} \\ \sum_{n=1}^{3} \Psi_n \, a_n \, \mathrm{e}^{-k_n (L - x_f)} \\ \sum_{n=1}^{3} k_n^2 \, a_n \, \mathrm{e}^{-k_n (L - x_f)} \\ \sum_{n=1}^{3} a_n \, \mathrm{e}^{-k_n (L - x_f)} \end{Bmatrix}. \tag{16}$$

Here $e_n = \mathrm{e}^{k_n L}$ and $e_{-n} = \mathrm{e}^{-k_n L}$.

The relevant matrix equations for clamped ends and free ends are given in Appendix A.

The necessary matrix equation for the determination of A_n values when there is warping constraint, for simply supported ends and a unit force P_z, is

$$
\begin{array}{r}
w(0): \\
w''(0): \\
\phi(0): \\
\phi''(0): \\
\phi''(L): \\
\phi(L): \\
w''(L): \\
w(L):
\end{array}
\begin{bmatrix}
1 & 1 & 1 & 1 & 1 & 1 & 1 & 1 \\
k_1^2 & k_1^2 & k_2^2 & k_2^2 & k_3^2 & k_3^2 & k_4^2 & k_4^2 \\
\Psi_1 & \Psi_1 & \Psi_2 & \Psi_2 & \Psi_3 & \Psi_3 & \Psi_4 & \Psi_4 \\
k_1^2\,\Psi_1 & k_1^2\,\Psi_1 & k_2^2\,\Psi_2 & k_2^2\,\Psi_2 & k_3^2\,\Psi_3 & k_3^2\,\Psi_3 & k_4^2\,\Psi_4 & k_4^2\,\Psi_4 \\
k_1^2\,\Psi_1\,e_1 & k_1^2\,\Psi_1\,e_{-1} & k_2^2\,\Psi_2\,e_2 & k_2^2\,\Psi_2\,e_{-2} & k_3^2\,\Psi_3\,e_3 & k_3^2\,\Psi_3\,e_{-3} & k_4^2\,\Psi_4\,e_4 & k_4^2\,\Psi_4\,e_{-4} \\
\Psi_1\,e_1 & \Psi_1\,e_{-1} & \Psi_2\,e_2 & \Psi_2\,e_{-2} & \Psi_3\,e_3 & \Psi_3\,e_{-3} & \Psi_4\,e_4 & \Psi_4\,e_{-4} \\
k_1^2\,e_1 & k_1^2\,e_{-1} & k_2^2\,e_2 & k_2^2\,e_{-2} & k_3^2\,e_3 & k_3^2\,e_{-3} & k_4^2\,e_4 & k_4^2\,e_{-4} \\
e_1 & e_{-1} & e_2 & e_{-2} & e_3 & e_{-3} & e_4 & e_{-4}
\end{bmatrix}
\begin{Bmatrix} A_1 \\ A_2 \\ A_3 \\ A_4 \\ A_5 \\ A_6 \\ A_7 \\ A_8 \end{Bmatrix}
= -
\begin{Bmatrix}
\sum_{n=1}^{4} a_n\,\mathrm{e}^{-k_n x_f} \\
\sum_{n=1}^{4} k_n^2\,a_n\,\mathrm{e}^{-k_n x_f} \\
\sum_{n=1}^{4} \Psi_n\,a_n\,\mathrm{e}^{-k_n x_f} \\
\sum_{n=1}^{4} k_n^2\,\Psi_n\,a_n\,\mathrm{e}^{-k_n x_f} \\
\sum_{n=1}^{4} k_n^2\,\Psi_n\,a_n\,\mathrm{e}^{-k_n (L - x_f)} \\
\sum_{n=1}^{4} \Psi_n\,a_n\,\mathrm{e}^{-k_n (L - x_f)} \\
\sum_{n=1}^{4} k_n^2\,a_n\,\mathrm{e}^{-k_n (L - x_f)} \\
\sum_{n=1}^{4} a_n\,\mathrm{e}^{-k_n (L - x_f)}
\end{Bmatrix}. \tag{17}
$$

Appendix A also gives the relevant matrix equations for clamped and free end cases in which there is warping constraint.

The required A_n values are numerically found from equations (16) or (17). Their substitution into equations (12) and (13) yields the required displacement response at any point of the beam.

2.3. TRIPLY COUPLED VIBRATIONS

In Figure 3 is shown a typical cross-section of no axial symmetry, representing a triply coupled case. In this case the flexural vibrations in the z direction, flexural vibrations in the y direction and the torsional vibrations are all coupled. The equations of motion for these types of coupled vibrations are known to be [1, 2]

$$EI_\xi \frac{\partial^4 w}{\partial x^4} + m\frac{\partial^2 w}{\partial t^2} + EI_{v\xi}\frac{\partial^4 v}{\partial x^4} + mc_y\frac{\partial^2 \phi}{\partial t^2} = 0, \qquad EI_v \frac{\partial^4 v}{\partial x^4} + m\frac{\partial^2 v}{\partial t^2} + EI_{v\xi}\frac{\partial^4 w}{\partial x^4} + mc_z\frac{\partial^2 \phi}{\partial t^2} = 0,$$

$$E\Gamma_0 \frac{\partial^4 \phi}{\partial x^4} - GJ\frac{\partial^2 \phi}{\partial x^2} + mc_y\frac{\partial^2 w}{\partial t^2} + mc_z\frac{\partial^2 v}{\partial t^2} + \rho I_0\frac{\partial^2 \phi}{\partial t^2} = 0. \tag{18}$$

In addition to the parameters already defined in section 2.2, v is the flexural displacement in the y direction, EI_v is the flexural stiffness in the y direction, $EI_{v\xi}$ is the coupling stiffness and c_z is the eccentricity between the centroid and the shear centre in the z direction.

If one assumes that

$$w(x, t) = w_n\, e^{k_n x}\, e^{i\omega t}, \qquad v(x, t) = v_n\, e^{k_n x}\, e^{i\omega t}, \qquad \phi(x, t) = \phi_n\, e^{k_n x}\, e^{i\omega t}, \tag{19}$$

substitution of these expressions into equations (18) gives the following equations for the

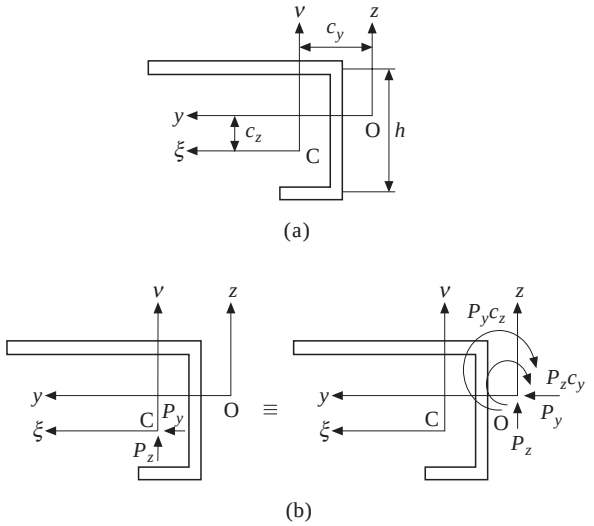

Figure 3. A typical cross-section of triple-coupling. (a) Co-ordinate system; (b) real and effective loadings.

wavenumbers:

$$(E\Gamma_0)\,[(EI_\xi)\,(EI_v) - (EI_{v\xi})^2]k_n^{12} - (GJ)\,[(EI_\xi)\,(EI_v) - (EI_{v\xi})^2]k_n^{10} - [(\rho I_0\,\omega^2)\,((EI_\xi)\,(EI_v)$$

$$-(EI_{v\xi})^2) + (E\Gamma_0)\,(m\omega^2)\,(EI_\xi + EI_v)]k_n^8 + (GJ)\,(m\omega^2)\,(EI_\xi + EI_v)k_n^6$$

$$-[(\rho I_0\,\omega^2)(m\omega^2)(EI_\xi + EI_v) + (E\Gamma_0)\,(m\omega^2)^2 - ((EI_\xi)c_z^2 + (EI_v)c_y^2 - (EI_{v\xi})c_z^2\,c_y^2)\,(m\omega^2)^2]k_n^4$$

$$-(GJ)\,(m\omega^2)^2k_n^2 + [(m\omega^2)^3(c_z^2 + c_y^2) - \rho I_0\,\omega^2(m\omega^2)^2] = 0. \tag{20}$$

This equation is of 12th order and defines 12 wavenumbers in six positive and negative pairs ($j = 6$). These waves are influenced by both the flexural and the torsional properties of the structure and describe the triply coupled motion charactertistics.

Note that the exclusion of warping constraint from the analysis reduces equation (20) to tenth order:

$$(GJ)[(EI_\xi)(EI_v) - (EI_{v\xi})^2]k_n^{10} + [(\rho I_0\omega^2)\{(EI_\xi)\,(EI_v) - (EI_{v\xi})^2\}]k_n^8 - (GJ)\,(m\omega^2)(EI_\xi + EI_v)k_n^6$$

$$+[(\rho I_0\,\omega^2)\,(m\omega^2)\,(EI_\xi + EI_v)^2 - \{(EI_\xi)c_z^2 + (EI_v)c_y^2 - (EI_{v\xi})c_z^2\,c_y^2\}\,(m\omega^2)^2]k_n^4$$

$$+(GJ)\,(m\omega^2)^2k_n^2 - [(m\omega^2)^3(c_z^2 + c_y^2) - \rho I_0\,\omega^2(m\omega^2)^2] = 0. \tag{21}$$

Equation (21) defines ten wavenumbers in five positive and negative pairs ($j = 5$). Following the theory outlined in section 2.2, one can conclude that a force P_z through the centroid will create the following forced waves at any $|\,x\,|$ along the length of the beam:

$$w(x, t) = P_z \sum_{n=1}^{j} a_n\,\mathrm{e}^{-k_n|\,x\,|}\,\mathrm{e}^{\mathrm{i}\omega t}, \qquad v(x, t) = P_z \sum_{n=1}^{j} b_n\,\mathrm{e}^{-k_n|\,x\,|}\,\mathrm{e}^{\mathrm{i}\omega t},$$

$$\phi(x, t) = P_z \sum_{n=1}^{j} c_n\,\mathrm{e}^{-k_n|\,x\,|}\,\mathrm{e}^{\mathrm{i}\omega t}. \tag{22}$$

The b_n and c_n values are found, by using equations (18) and (19), to be

$$b_n = \Pi_n\,a_n, \qquad \Pi_n = \frac{(EI_\xi\,k_n^4 - m\omega^2)\,(E\Gamma_0\,k_n^4 - GJk_n^2 - \rho I_0\,\omega^2) - (-c_y\,m\omega^2)^2}{(-c_y\,m\omega^2)\,(-c_z\,m\omega^2) - (EI_{v\xi}\,k_n^4)\,(E\Gamma_0\,k_n^4 - GJk_n^2 - \rho I_0\,\omega^2)},$$

$$c_n = \Phi_n\,a_n, \qquad \Phi_n = \frac{(EI_\xi\,k_n^4 - m\omega^2)\,(EI_v\,k_n^4 - m\omega^2) - (EI_{v\xi}\,k_n^4)^2}{(EI_{v\xi}\,k_n^4)\,(-c_z\,m\omega^2) - (-c_y\,m\omega^2)\,(EI_v\,k_n^4 - m\omega^2)}. \tag{23}$$

The a_n values can be found by satisfying the following compatibility and continuity conditions:

$$EI_\xi\,\partial^3 w(x, t)/\partial x^3\,|_{x=0} + EI_{v\xi}\,\partial^3 v(x, t)/\partial x^3\,|_{x=0} = P_z\,/2, \qquad \partial w(x, t)/\partial x\,|_{x=0} = 0,$$

$$EI_v\,\partial^3 v(x, t)/\partial x^3\,|_{x=0} + EI_{v\xi}\,\partial^3 w(x, t)/\partial x^3\,|_{x=0} = 0, \qquad \partial v(x, t)/\partial x\,|_{x=0} = 0,$$

$$GJ\,\partial\phi(x, t)/\partial x\,|_{x=0} - E\Gamma_0\,\partial^3\phi(x, t)/\partial x^3\,|_{x=0} = P_z\,c_y\,/2, \qquad \partial\phi(x, t)/\partial x\,|_{x=0} = 0. \tag{24}$$

Equations (22), (23) and (24) result in a sixth order matrix equation which, through numerical solution, yields the a_n values.

In the absence of the warping constraint, equations (24) become

$$EI_\xi\,\partial^3 w(x,t)/\partial x^3\,|_{x=0} + EI_{v\xi}\,\partial^3 v(x,t)/\partial x^3\,|_{x=0} = P_z\,/2, \qquad \partial w(x,t)/\partial x\,|_{x=0} = 0,$$

$$EI_v\,\partial^3 v(x,t)/\partial x^3\,|_{x=0} + EI_{v\xi}\,\partial^3 w(x,t)/\partial x^3\,|_{x=0} = 0, \qquad \partial v(x,t)/\partial x\,|_{x=0} = 0,$$

$$GJ\,\partial\phi(x,t)/\partial x\,|_{x=0} = P_z\,c_y\,/2. \tag{25}$$

Now equations (22), (23) and (25) give a fifth order matrix equation for the a_n values. If the force is applied only as P_y, equations (24) become

$$EI_\xi\,\partial^3 w(x,t)/\partial x^3\,|_{x=0} + EI_{v\xi}\,\partial^3 v(x,t)/\partial x^3\,|_{x=0} = 0, \qquad \partial w(x,t)/\partial x\,|_{x=0} = 0,$$

$$EI_v\,\partial^3 v(x,t)/\partial x^3\,|_{x=0} + EI_{v\xi}\,\partial^3 w(x,t)/\partial x^3\,|_{x=0} = P_y\,/2, \qquad \partial v(x,t)/\partial x\,|_{x=0} = 0,$$

$$GJ\,\partial\phi(x,t)/\partial x\,|_{x=0} - E\Gamma_0\,\partial^3\phi(x,t)/\partial x^3\,|_{x=0} = P_y\,c_z\,/2, \qquad \partial\phi(x,t)/\partial x\,|_{x=0} = 0. \tag{26}$$

If both P_y and P_z are applied simultaneously, depending on the admission of warping constraint, the required conditions should be provided by considering equations (24), (25) and (26).

Consideration of $2j$ free waves as well gives the total transverse displacements due to P_z as

$$w(x,t) = \left(\sum_{n=1}^{2j} \mathrm{e}^{k_n x} A_n + P_z \sum_{n=1}^{j} a_n\,\mathrm{e}^{-k_n|x-x_f|}\right)\mathrm{e}^{\mathrm{i}\omega t},$$

$$v(x,t) = \left(\sum_{n=1}^{2j} \mathrm{e}^{k_n x} \Pi_n\,A_n + P_z \sum_{n=1}^{j} \Pi_n\,a_n\,\mathrm{e}^{-k_n|x-x_f|}\right)\mathrm{e}^{\mathrm{i}\omega t},$$

$$\phi(x,t)\left(\sum_{n=1}^{2j} \mathrm{e}^{k_n x} \Phi_n\,A_n + P_z \sum_{n=1}^{j} \Phi_n\,a_n\,\mathrm{e}^{-k_n|x-x_f|}\right)\mathrm{e}^{\mathrm{i}\omega t}. \tag{27}$$

If required, the warping displacement can be found as

$$u(x,t) = -2A_s\frac{\partial\phi(x,t)}{\partial x} = -2A_s\left(\sum_{n=1}^{2j} \mathrm{e}^{k_n x} k_n\,\Phi_n\,A_n - P_z \sum_{n=1}^{j} k_n\,\Phi_n\,a_n\,\mathrm{e}^{-k_n|x-x_f|}\right)\mathrm{e}^{\mathrm{i}\omega t}. \tag{28}$$

The A_n values are again found by satisfying the necessary $2j$ end boundary conditions. For simply supported ends, and for $EI_{v\xi} = 0$, they are known to be

$$j = 5, \quad w(0) = w(L) = w''(0) = w''(L) = v(0) = v(L) = v''(0) = v''(L) = \phi(0) = \phi(L) = 0,$$

$$j = 6, \quad w(0) = w(L) = w''(0) = w''(L) = v(0) = v(L) = v''(0) = v''(L)$$

$$= \phi(0) = \phi(L) = \phi''(0) = \phi''(L) = 0. \tag{29}$$

If equations (27) (and also equation (28) if warping constraint is included) are substituted into the relevant equations (29), a matrix equation is obtained. The order of the matrix equation is ten for the no warping constraint case and twelve for the case in which the warping constraint is included. The A_n values, respectively, are then numerically found from the following equations; their substitution into equations (27) and (28) gives the required displacement response at any point of the beam:

$$
\begin{array}{c}
\\
w(0): \\
v(0): \\
w''(0): \\
v''(0): \\
\phi(0): \\
\phi(L): \\
v''(L): \\
w''(L): \\
v(L): \\
w(L):
\end{array}
\begin{bmatrix}
1 & 1 & 1 & 1 & 1 & 1 & 1 & 1 & 1 & 1 \\
\Pi_1 & \Pi_1 & \Pi_2 & \Pi_2 & \Pi_3 & \Pi_3 & \Pi_4 & \Pi_4 & \Pi_5 & \Pi_5 \\
k_1^2 & k_1^2 & k_2^2 & k_2^2 & k_3^2 & k_3^2 & k_4^2 & k_4^2 & k_5^2 & k_5^2 \\
k_1^2\Pi_1 & k_1^2\Pi_1 & k_2^2\Pi_2 & k_2^2\Pi_2 & k_3^2\Pi_3 & k_3^2\Pi_3 & k_4^2\Pi_4 & k_4^2\Pi_4 & k_5^2\Pi_5 & k_5^2\Pi_5 \\
\Phi_1 & \Phi_1 & \Phi_2 & \Phi_2 & \Phi_3 & \Phi_3 & \Phi_4 & \Phi_4 & \Phi_5 & \Phi_5 \\
\Phi_1 e_1 & \Phi_1 e_{-1} & \Phi_2 e_2 & \Phi_2 e_{-2} & \Phi_3 e_3 & \Phi_3 e_{-3} & \Phi_4 e_4 & \Phi_4 e_{-4} & \Phi_5 e_5 & \Phi_5 e_{-5} \\
k_1^2\Pi_1 e_1 & k_1^2\Pi_1 e_{-1} & k_2^2\Pi_2 e_2 & k_2^2\Pi_2 e_{-2} & k_3^2\Pi_3 e_3 & k_3^2\Pi_3 e_{-3} & k_4^2\Pi_4 e_4 & k_4^2\Pi_4 e_{-4} & k_5^2\Pi_5 e_5 & k_5^2\Pi_5 e_{-5} \\
k_1^2 e_1 & k_1^2 e_{-1} & k_2^2 e_2 & k_2^2 e_{-2} & k_3^2 e_3 & k_3^2 e_{-3} & k_4^2 e_4 & k_4^2 e_{-4} & k_5^2 e_5 & k_5^2 e_{-5} \\
\Pi_1 e_1 & \Pi_1 e_{-1} & \Pi_2 e_2 & \Pi_2 e_{-2} & \Pi_3 e_3 & \Pi_3 e_{-3} & \Pi_4 e_4 & \Pi_4 e_{-4} & \Pi_5 e_5 & \Pi_5 e_{-5} \\
e_1 & e_{-1} & e_2 & e_{-2} & e_3 & e_{-3} & e_4 & e_{-4} & e_5 & e_{-5}
\end{bmatrix}
\begin{Bmatrix} A_1 \\ A_2 \\ A_3 \\ A_4 \\ A_5 \\ A_6 \\ A_7 \\ A_8 \\ A_9 \\ A_{10} \end{Bmatrix}
=
-
\begin{Bmatrix}
\sum_{n=1}^{5} a_n e^{-k_n x_f} \\
\sum_{n=1}^{5} \Pi_n a_n e^{-k_n x_f} \\
\sum_{n=1}^{5} k_n^2 a_n e^{-k_n x_f} \\
\sum_{n=1}^{5} k_n^2 \Pi_n a_n e^{-k_n x_f} \\
\sum_{n=1}^{5} \Phi_n a_n e^{-k_n x_f} \\
\sum_{n=1}^{5} \Phi_n a_n e^{-k_n (L - x_f)} \\
\sum_{n=1}^{5} k_n^2 \Pi_n a_n e^{-k_n (L - x_f)} \\
\sum_{n=1}^{5} k_n^2 a_n e^{-k_n (L - x_f)} \\
\sum_{n=1}^{5} \Pi_n a_n e^{-k_n (L - x_f)} \\
\sum_{1}^{5} a_n e^{-k_n (L - x_f)}
\end{Bmatrix}
\tag{30}
$$

$$
\begin{array}{r}
w(0)\text{:}\\ v(0)\text{:}\\ w''(0)\text{:}\\ v''(0)\text{:}\\ \phi(0)\text{:}\\ \phi''(0)\text{:}\\ \phi''(L)\text{:}\\ \phi(L)\text{:}\\ v''(L)\text{:}\\ w''(L)\text{:}\\ v(L)\text{:}\\ w(L)\text{:}
\end{array}
\begin{bmatrix}
1 & 1 & 1 & 1 & 1 & 1 & 1 & 1 & 1 & 1 & 1 & 1\\
\Pi_1 & \Pi_1 & \Pi_2 & \Pi_2 & \Pi_3 & \Pi_3 & \Pi_4 & \Pi_4 & \Pi_5 & \Pi_5 & \Pi_6 & \Pi_6\\
k_1^2 & k_1^2 & k_2^2 & k_2^2 & k_3^2 & k_3^2 & k_4^2 & k_4^2 & k_5^2 & k_5^2 & k_6^2 & k_6^2\\
k_1^2\,\Pi_1 & k_1^2\,\Pi_1 & k_2^2\,\Pi_2 & k_2^2\,\Pi_2 & k_3^2\,\Pi_3 & k_3^2\,\Pi_3 & k_4^2\,\Pi_4 & k_4^2\,\Pi_4 & k_5^2\,\Pi_5 & k_5^2\,\Pi_5 & k_6^2\,\Pi_6 & k_6^2\,\Pi_6\\
\Phi_1 & \Phi_1 & \Phi_2 & \Phi_2 & \Phi_3 & \Phi_3 & \Phi_4 & \Phi_4 & \Phi_5 & \Phi_5 & \Phi_6 & \Phi_6\\
k_1^2\,\Phi_1 & k_1^2\,\Phi_1 & k_2^2\,\Phi_2 & k_2^2\,\Phi_2 & k_3^2\,\Phi_3 & k_3^2\,\Phi_3 & k_4^2\,\Phi_4 & k_4^2\,\Phi_4 & k_5^2\,\Phi_5 & k_5^2\,\Phi_5 & k_6^2\,\Phi_6 & k_6^2\,\Phi_6\\
k_1^2\,\Phi_1\,e_1 & k_1^2\,\Phi_1\,e_{-1} & k_2^2\,\Phi_2\,e_2 & k_2^2\,\Phi_2\,e_{-2} & k_3^2\,\Phi_3\,e_3 & k_3^2\,\Phi_3\,e_{-3} & k_4^2\,\Phi_4\,e_4 & k_4^2\,\Phi_4\,e_{-4} & k_5^2\,\Phi_5\,e_5 & k_5^2\,\Phi_5\,e_{-5} & k_6^2\,\Phi_6\,e_6 & k_6^2\,\Phi_6\,e_{-6}\\
\Phi_1\,e_1 & \Phi_1\,e_{-1} & \Phi_2\,e_2 & \Phi_2\,e_{-2} & \Phi_3\,e_3 & \Phi_3\,e_{-3} & \Phi_4\,e_4 & \Phi_4\,e_{-4} & \Phi_5\,e_5 & \Phi_5\,e_{-5} & \Phi_6\,e_6 & \Phi_6\,e_{-6}\\
k_1^2\,\Pi_1\,e_1 & k_1^2\,\Pi_1\,e_{-1} & k_2^2\,\Pi_2\,e_2 & k_2^2\,\Pi_2\,e_{-2} & k_3^2\,\Pi_3\,e_3 & k_3^2\,\Pi_3\,e_{-3} & k_4^2\,\Pi_4\,e_4 & k_4^2\,\Pi_4\,e_{-4} & k_5^2\,\Pi_5\,e_5 & k_5^2\,\Pi_5\,e_{-5} & k_6^2\,\Pi_6\,e_6 & k_6^2\,\Pi_6\,e_{-6}\\
k_1^2\,e_1 & k_1^2\,e_{-1} & k_2^2\,e_2 & k_2^2\,e_{-2} & k_3^2\,e_3 & k_3^2\,e_{-3} & k_4^2\,e_4 & k_4^2\,e_{-4} & k_5^2\,e_5 & k_5^2\,e_{-5} & k_6^2\,e_6 & k_6^2\,e_{-6}\\
\Pi_1\,e_1 & \Pi_1\,e_{-1} & \Pi_2\,e_2 & \Pi_2\,e_{-2} & \Pi_3\,e_3 & \Pi_3\,e_{-3} & \Pi_4\,e_4 & \Pi_4\,e_{-4} & \Pi_5\,e_5 & \Pi_5\,e_{-5} & \Pi_6\,e_6 & \Pi_6\,e_{-6}\\
e_1 & e_{-1} & e_2 & e_{-2} & e_3 & e_{-3} & e_4 & e_{-4} & e_5 & e_{-5} & e_6 & e_{-6}
\end{bmatrix}
\begin{Bmatrix} A_1\\ A_2\\ A_3\\ A_4\\ A_5\\ A_6\\ A_7\\ A_8\\ A_9\\ A_{10}\\ A_{11}\\ A_{12} \end{Bmatrix}
= -
\begin{Bmatrix}
\sum_{n=1}^{6} a_n \mathrm{e}^{-k_n x_f}\\
\sum_{n=1}^{6} a_n \Pi_n \mathrm{e}^{-k_n x_f}\\
\sum_{n=1}^{6} k_n^2 a_n \mathrm{e}^{-k_n x_f}\\
\sum_{n=1}^{6} k_n^2 a_n \Pi_n \mathrm{e}^{-k_n x_f}\\
\sum_{n=1}^{6} a_n \Phi_n \mathrm{e}^{-k_n x_f}\\
\sum_{n=1}^{6} k_n^2 \Phi_n a_n \mathrm{e}^{-k_n x_f}\\
\sum_{n=1}^{6} k_n^2 \Phi_n a_n \mathrm{e}^{-k_n (L - x_f)}\\
\sum_{n=1}^{6} a_n \Phi_n \mathrm{e}^{-k_n (L - x_f)}\\
\sum_{n=1}^{6} k_n^2\, a_n\, \Pi_n\, \mathrm{e}^{-k_n (L - x_f)}\\
\sum_{n=1}^{6} k_n^2\, a_n\, \mathrm{e}^{-k_n (L - x_f)}\\
\sum_{n=1}^{6} a_n\, \Pi_n\, \mathrm{e}^{-k_n (L - x_f)}\\
\sum_{n=1}^{6} a_n\, \mathrm{e}^{-k_n (L - x_f)}
\end{Bmatrix}. \tag{31}
$$

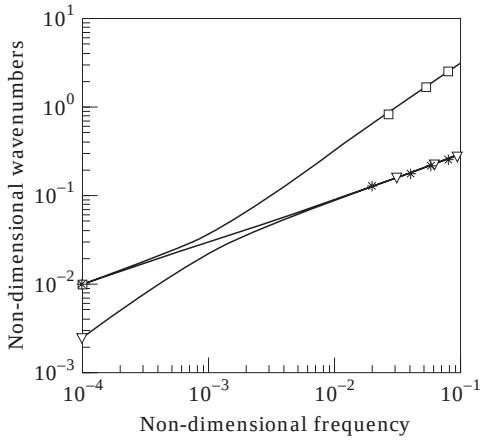

Figure 4. Coupled wavenumbers: $\eta = 0$, $\eta_t = 0$, double-coupling, no warping constraint. –∗–, Real part (k_2); –□–, imaginary part (k_1); –▽–, imaginary part (k_3).

3. RESULTS AND DISCUSSION

The theoretical models used in the study have the following geometric and material properties; the cross-sections of the models are those given in Figures 2 and 3: double-coupling, $L = 1$ (m), $A = 1{\cdot}0 \times 10^{-4}$ (m^2), $h = 5{\cdot}0 \times 10^{-2}$ (m), $I_\xi = 4{\cdot}17 \times 10^{-8}$ (m^4), $c_y = 15{\cdot}625 \times 10^{-3}$ (m), $J = 3{\cdot}33 \times 10^{-11}$ (m^3), $I_0 = 7{\cdot}26 \times 10^{-8}$ (m^4), $\rho = 2700$ (kg/m^3), $E = 7 \times 10^{10}$ (N/m^2), $G = 2{\cdot}6 \times 10^{10}$ (N/m^2), $\Gamma_0 = 2{\cdot}85 \times 10^{-12}$ (m^6); triple-coupling, $L = 1$ (m), $A = 9{\cdot}68 \times 10^{-5}$ (m^2), $h = 38{\cdot}10 \times 10^{-3}$ (m), $I_v = 5{\cdot}08 \times 10^{-9}$ (m^4), $I_\xi = 2{\cdot}24 \times 10^{-8}$ (m^4), $I_{v\xi} = 4{\cdot}25 \times 10^{-9}$ (m^4), $c_y = 10{\cdot}43 \times 10^{-3}$ (m), $c_z = 9{\cdot}09 \times 10^{-3}$ (m), $J = 5{\cdot}20 \times 10^{-11}$ (m^3), $I_0 = 4{\cdot}60 \times 10^{-8}$ (m^4), $\rho = 2700$ (kg/m^3), $E = 7 \times 10^{10}$ (N/m^2), $G = 2{\cdot}6 \times 10^{10}$ (N/m^2), $\Gamma_0 = 7{\cdot}11 \times 10^{-12}$ (m^6). The structural damping is included through the flexural stiffnesses as $EI_\xi = EI_\xi\,(1 + \mathrm{i}\eta)$, $EI_v = EI_v\,(1 + \mathrm{i}\eta)$ and through the torsional stiffness as $GJ = GJ(1 + \mathrm{i}\eta_t)$.

3.1. COUPLED WAVENUMBERS

The first part of this section gives the detailed analysis of the coupled wavenumbers. The wavenumbers are plotted in non-dimensional form and the following non-dimensional parameters are used: ND wavenumber, $(h)k_n$; ND frequency, $(2\pi h^2(\rho A/EI_\xi)^{1/2})f$.

It has long been known that if an Euler–Bernoulli beam is harmonically excited at a point and if it undergoes pure bending then in each direction two waves travel away from the point of excitation. If the beam is undamped, one of those waves has a purely real wavenumber and the other one has a purely imaginary wavenumber. Both of those wavenumbers are identical in magnitude ($k_b = (m\omega^2/EI_\xi)^{1/4}$) for each frequency. If the vibrations are of undamped purely torsional type and if the warping constraint is omitted, then in each direction one wave travels away from the point of application of the harmonic torque which has a purely imaginary wavenumber ($k_t = (-\rho I_0\,\omega^2/GJ)^{1/2}$). In the context of wave propagation, a purely imaginary wavenumber corresponds to a propagating wave, whereas a purely real wavenumber to a non-propagating wave.

In Figure 4 are represented the non-zero components of wavenumbers of the waves in the doubly coupled system for zero damping. The warping constraint is excluded from the analysis. This means that the wavenumber equation is sixth order and the wavenumbers are found from equation (7). Now, since the flexural vibrations in the z direction and torsional vibrations are coupled, one expects altogether three waves to travel in each

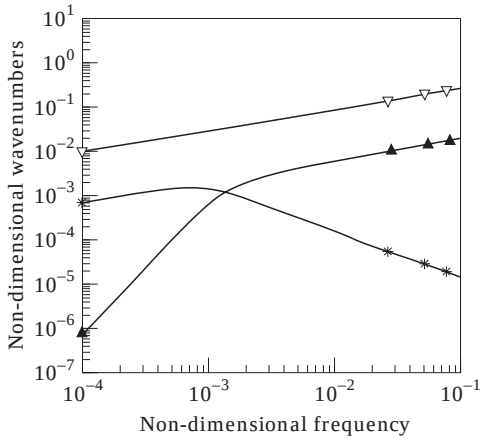

Figure 5. Real parts of coupled wavenumbers: $\eta = 0{\cdot}3$, $\eta_t = 0$, double-coupling, no warping constraint. $-*-$, k_1; $-\triangledown-$, k_2; $-\blacktriangle-$, k_3.

direction. This is indeed true and is shown in Figure 4, but now due to coupling effects each wave is affected. The curve for the real wavenumber k_2 represents an evanescent wave which has mainly flexural with some torsional character. The curve for the imaginary wavenumber k_3 represents a propagating wave which is predominantly flexural but with some torsion. Although both are flexural, due to the existing coupling, they no longer have identical magnitudes such as those wavenumbers of uncoupled, undamped flexural waves. The curve which belongs to the imaginary wavenumber k_1 represents a propagating wave which is predominantly torsional with some bending.

If the structural damping is included in the analysis, all the wavenumbers become complex. This indicates that each wave attenuates with distance travelled and each wave propagates energy to some extent. This feature can be seen in Figures 5 and 6 which respectively represent the real parts and the imaginary parts of the wavenumbers of double-coupling for $\eta = 0{\cdot}3$ and $\eta_t = 0$. The warping constraint is again excluded. Now each wavenumber has both real and imaginary parts. Furthermore, the parts which did exist for $\eta = 0$ and $\eta_t = 0$ have not changed significantly in magnitude.

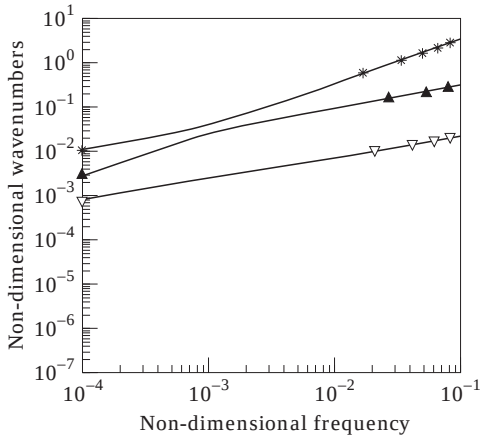

Figure 6. Imaginary parts of coupled wavenumbers: $\eta = 0{\cdot}3$, $\eta_t = 0$, double-coupling, no warping constraint. Key as Figure 5.

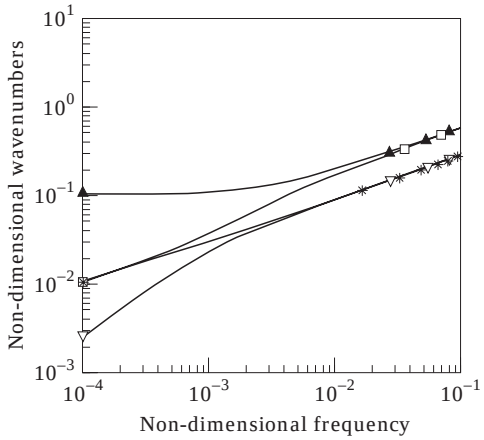

Figure 7. Coupled wavenumbers: $\eta = 0$, $\eta_t = 0$, double-coupling, warping constraint included. –▲–, Real part (k_1); –∗–, real part (k_3); –□–, imaginary part (k_2); –▽–, imaginary part (k_4).

The effect of the warping constraint on the wavenumbers is also considered and the resulting wavenumber components are given in Figure 7 for no damping. Only non-zero components are shown. The wavenumbers are found from equation (6). In the case of no damping, the inclusion of warping constraint introduces a new wave which is evanescent in nature. The wavenumber of this wave is designated as k_1 in Figure 7. In the same figure, the imaginary wavenumber k_2 belongs to a predominantly torsional wave. The predominantly flexural, evanescent and propagating waves are represented by the wavenumbers k_3 and k_4 respectively. The consideration of the warping constraint basically modifies the magnitude of wavenumber k_2 and reduces it considerably, especially at higher frequencies. This can better be seen if one compares Figures 4 and 7. It is apparent that the admission of warping constraint prevents the predominantly torsional wave propagation mechanism with increasing frequency.

The characteristics of the wavenumbers of triple-coupling are given in Figures 8 and 9

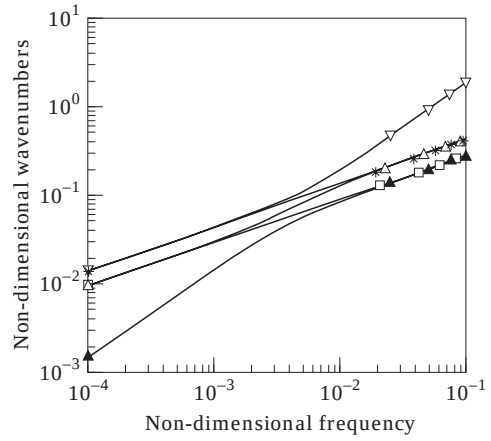

Figure 8. Coupled wavenumbers: $\eta = 0$, $\eta_t = 0$, triple-coupling, only mass coupling, no warping constraint. –∗–, Real part (k_2); –□–, real part (k_4); –▽–, imaginary part (k_1); –△–, imaginary part (k_3); –▲–, imaginary part (k_5).

for no damping. The graphs show, respectively, the cases in which only the mass coupling is considered and both mass and stiffness couplings are taken into consideration. In both figures, effects of the warping constraint are neglected. Equation (21) is used to determine the wavenumbers. The graphs are very similar in their trends and at first glance they look as though coupling stiffness has no additional effect at all on the wavenumbers. The actual reason stems from the fact that the cross-section considered has a small coupling stiffness.

In Figures 8 and 9, five distinct wavenumbers group to become three at the extreme frequencies of the ranges considered. In this case, the flexural properties in the y and z direction and the torsional properties all affect each other. In both figures, the wavenumber k_1 represents a predominantly torsional wave with some bi-directional flexural properties. The wavenumbers k_2 and k_3 represent the vertical bending waves (in the z direction), being evanescent and propagating respectively. The wavenumbers k_4 and k_5 represent the evanescent and propagating lateral bending waves. All the waves defined by wavenumbers k_2–k_5 are predominantly flexural with some torsion. For the case considered, the lateral, purely flexural waves have smaller wavenumbers than the vertical, purely flexural waves. This feature reflects itself in the existence of the triple-coupling as well, especially at higher frequencies.

Finally, the most general case of the triple-coupling is considered. Now as well as mass and stiffness couplings, the warping constraint is also assumed to exist. By using equation (20) 12 wavenumbers, in groups of six, are obtained. The non-zero components of the wavenumbers of the six waves, for no damping, are given in Figure 10. The wavenumbers and the corresponding waves they represent are classified as follows. k_1 represents the evanescent wave due to warping constraint. k_2 represents the propagating wave which is predominantly torsional. k_3 and k_4 are the wavenumbers of evanescent and propagating, predominantly flexural, waves of vertical bending (in the z direction). The evanescent and propagating waves of lateral bending are characterized by the wavenumbers k_5 and k_6. These waves are also predominantly flexural. At low frequencies there are four groups, but as frequency increases, the wavenumbers group into three and, as in the case of double-coupling, the newly introduced wave affects the predominantly torsional wave characteristics.

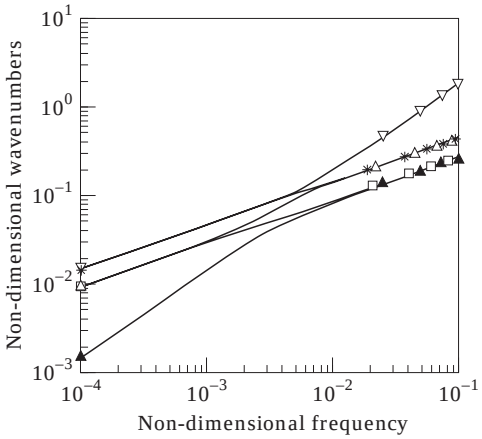

Figure 9. Coupled wavenumbers: $\eta = 0$, $\eta_t = 0$, triple-coupling, mass and stiffness coupling, no warping constraint. Key as Figure 8.

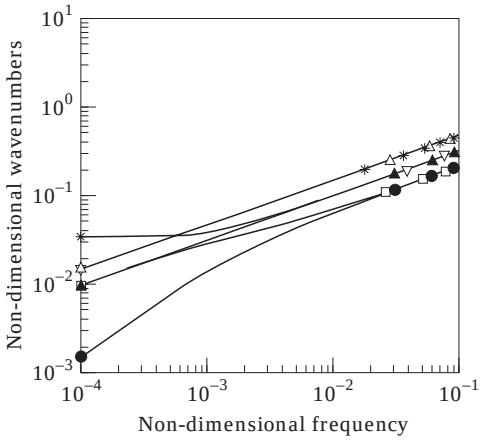

Figure 10. Coupled wavenumbers: $\eta = 0$, $\eta_t = 0$, triple-coupling, mass and stiffness coupling, warping constraint included. –∗–, Real part (k_1); –▽–, real part (k_3); –□–, real part (k_5); –△–, imaginary part (k_2); –▲–, imaginary part (k_4); –●–, imaginary part (k_6).

3.2. COUPLED FREQUENCY RESPONSES

3.2.1. *Doubly coupled channels*

The second part of the analysis is focused on the frequency response characteristics of the channels. First, the validity of the proposed method is verified. Since the exact data given in the literature is scarce, the verification process is done only for doubly coupled channels. The first validation has been achieved by determining the natural frequencies of simply supported channels by the methods given in reference [9]. Those values are then

TABLE 1

The coupled resonance frequenices (Hz) *of doubly coupled channel* (*simply supported ends*; T, *Torsional*; B, *bending in the z direction*; *current method*; $\eta = 10^{-6}$, $\eta_t = 10^{-6}$, *Reference* [9] = *undamped*)

No warping constraint		Warping constraint included	
Current method	Reference [9]	Current method	Reference [9]
33·01 (1.T)	33·01	58·68 (1.T)	58·68
66·37 (2.T)	66·37	205·34 (1.B)	205·34
99·66 (3.T)	99·66	207·27 (2.T)	207·27
132·92 (4.T)	132·92	453·79 (3.T)	453·79
166·18 (5.T)	166·18		
199·43 (6.T)	199·43		
201·84 (1.B)	201·84		
232·69 (7.T)	232·69		
265·93 (8.T)	265·93		
299·18 (9.T)	299·18		
332·43 (10.T)	332·43		
365·67 (11.T)	365·67		
398·92 (12.T)	398·92		
432·17 (13.T)	432·17		
465·41 (14.T)	465·41		
498·66 (15.T)	498·66		

TABLE 2

The coupled resonance frequenices (Hz) *of a turbine blade* (*no warping constraint*; *current method*; $\eta = 10^{-6}$, $\eta_t = 10^{-6}$, *Reference* [4] = *undamped*)

Current method	Reference [4]
144·56	144·65
903·82	904·37
1698·30	1699·31
2523·38	2524·92
4903·95	4906·92
5114·72	5117·77

compared to the resonance frequencies found from the developed method. The resonance frequenices are precisely located by allowing a very low damping ($\eta = 10^{-6}$, $\eta_t = 10^{-6}$) in the proposed theory. These virtually undamped resonance frequencies and the theoretical natural frequenices of reference [9] are given in Table 1 for a frequency range of 0–500 Hz. The results show extremely good agreement and this proves the accuracy of the proposed method.

In this respect, a fixed–free beam representing a turbine blade is also analyzed. In Table 2, the resonance frequencies obtained from the current method are compared to those given in reference [4].

A final comparison is made for the resonance frequenices of a free–free beam having warping constraint. The frequencies found from the developed method and the frequenices given in reference [5] are presented in Table 3. All of the data about the channels can be found in the relevant reference.

The agreement shown in Tables 2 and 3 is another indication of the correctness and the applicability of proposed method.

Bishop *et al*. [5] compared their results to those of other methods and expressed the view that their method was a convenient alternative to more complicated methods such as Vlasov theory and the finite element method. A similar argument can also be pursued about the proposed method. It is believed that its applicability to problems involving triple-coupling further enhances the features of the proposed method.

The case considered in Table 3 presented in graphical form is first. The forced frequency response of the free–free beam is plotted and is shown in Figure 11. Predominantly flexural, transfer transverse receptance (transverse displacement/transverse force) is found by using equation (12). The beam is excited at $x_f = 0{\cdot}13579$ m and the response is computed at

TABLE 3

The coupled resonance frequenices (rad/s) *of a free–free beam* (*warping constraint*; *current method*; $\eta = 10^{-6}$, $\eta_t = 10^{-6}$, *Reference* [5] = *undamped*)

Current method	Reference [5]
342·21	342·13
372·38	371·62
721·40	721·16
1247·47	1247·0
1791·99	1788·6
1970·39	1969·8

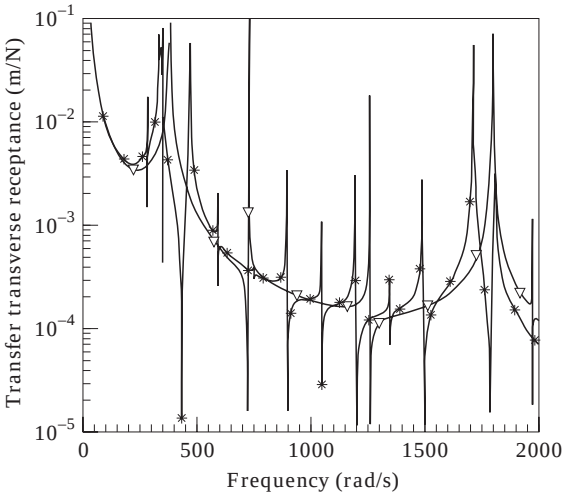

Figure 11. The transfer frequency responses of free–free doubly coupled beam: $\eta = 0{\cdot}01$, $\eta_t = 0{\cdot}001$, $x_f = 0{\cdot}13579$ m, $x = 0{\cdot}97531$ m, transverse frequency receptance w/P_z. –∗–, no warping constraint; –▽–, warping constraint.

$x = 0{\cdot}97531$ m. These rather strange excitation and response points are chosen intentionally, in order not to encounter a possible node within the frequency range of interest. Flexural and torsional damping values are assigned, respectively, as $\eta = 0{\cdot}01$ and $\eta_t = 0{\cdot}001$. In order to highlight the importance of the effects of the warping constraint, the frequency response of the beam having the same end boundary conditions and the properties but with no warping constraint is also plotted on the same figure.

The frequency response curves of the doubly coupled beam for simply supported, and clamped end conditions are given in Figures 12 and 13. The predominantly flexural response values are computed from equation (12) for $\eta = 0{\cdot}01$ and $\eta_t = 0{\cdot}001$. These

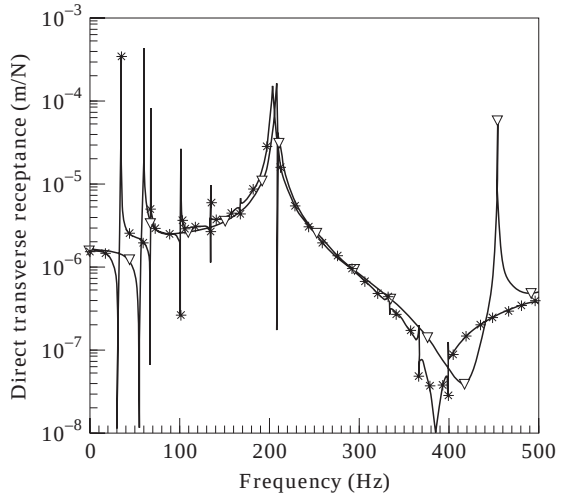

Figure 12. The direct frequency responses of simply supported doubly coupled beam: $\eta = 0{\cdot}01$, $\eta_t = 0{\cdot}001$, $x = 0{\cdot}13579$ m, w/P_z. –∗–, No warping constraint; –▽–, warping constraint.

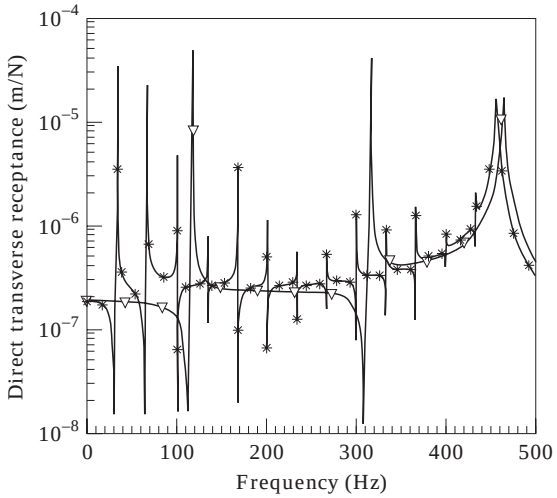

Figure 13. The direct frequency responses of clamped–clamped doubly coupled beam: $\eta = 0{\cdot}01$, $\eta_t = 0{\cdot}001$, $x = 0{\cdot}13579$ m, w/P_z. Key as Figure 12.

figures also illustrate the comparison of the cases in which either the warping constraint is considered or not. Direct transverse receptance values are computed at $x = 0{\cdot}13579$ (m).

It can be seen in all the figures concerned that when the warping is constrained the beam becomes stiffer, so fewer resonance frequencies are found in the same frequency range than when warping is free. For the cases in which there is no warping constraint, at flexural resonance frequencies one can observe a well behaved bending resonance behaviour, whereas the torsional resonance frequencies occur like spikes and at regular intervals. This indicates that the selected cross-sectional parameters result in a light coupling between the bending and the torsional motions. On the other hand, if the warping is constrained, the torsion dominated resonance frequencies no longer occur at equal intervals.

The theoretical beam, the cross-section of which is given in Figure 2, is then taken to be free–free and the resonance frequencies are precisely located for $\eta = 10^{-6}$ and $\eta_t = 10^{-6}$. The warping mode shapes of the beam at relevant resonance frequencies are shown in Figure 14. Free ends are modelled as if the end cross-sections are free to warp and free to twist. Hence one may expect to obtain the mode shapes of a free–free beam. A closer inspection of Figure 14 yields that this is indeed true for the frequencies of 132·57 Hz, 325·76 Hz and 465·34 Hz which represent the first and second torsion dominated resonances and the first bending dominated resonance in order. However, at 44·58 Hz a different form of behaviour is observed.

The bending, torsional and warping shapes at 44·58 Hz are given in Figure 15, which indicates a rigid-body-like mode.

The warping shapes of the free–free beam, at the first resonance frequenices of the beams having the indicated lengths are shown in Figure 16. All the other parameters of the study are kept constant. It can be seen that as the length is reduced, the shape becomes more straight.

3.2.2. *Triply coupled channels*

The coupled, predominantly flexural direct transverse receptances of the triply coupled beam are shown in Figure 17. The responses are computed at $x = 0{\cdot}13579$ (m). The calculations are made by using equation (27). $\eta = 0{\cdot}01$ and $\eta_t = 0{\cdot}001$ are assigned as damping coefficients. Only the mass coupling characteristics are included. The stiffness

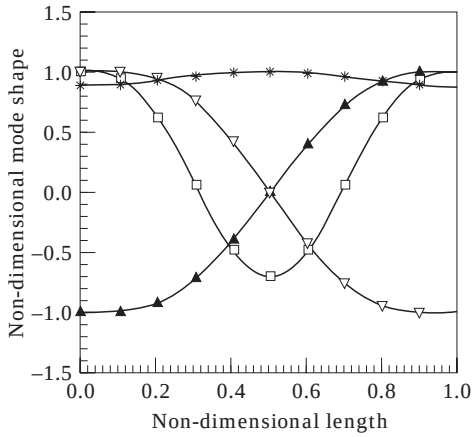

Figure 14. The warping mode shapes of free–free doubly coupled beam: $\eta = 0$, $\eta_t = 0$, P_z excitation. –∗–, 44·58 Hz; –▲–, 132·37 Hz; –□–, 325·76 Hz; –▽–, 465·34 Hz.

coupling terms and the effects of warping constraint are ignored. The resonance frequencies at 45·49 Hz, 101·73 Hz, 154·79 Hz, 207·43 Hz and 259·89 Hz are torsion dominated resonance frequencies, and the resonance frequencies at 69·91 Hz, 149·82 Hz at 257·29 Hz are bending dominated resonance frequenices.

The combined effects of the mass and stiffness couplings are computed and compared to the effects of mass coupling alone in Figure 18. It shows the transverse direct receptance in the z direction (w/P_z). It can be seen from Figure 18 that consideration of the coupling stiffness is found to affect the bending dominated resonance frequency, but has no significant effect on the values of the torsion dominated resonance frequencies.

The frequency responses of the most general case are shown in Figure 19. Now, in addition to the mass and stiffness couplings, the effects of the warping constraint are also considered. The extreme ends are taken as simply supported. The direct receptances are calculated from equation (27) for $\eta = 0{\cdot}01$ and $\eta_t = 0{\cdot}001$. The resonance frequencies at 51·87 Hz and 207·41 Hz are torsion dominated resonance frequencies, and the resonance frequencies at 114·79 Hz and 263·88 Hz are bending dominated resonance frequencies.

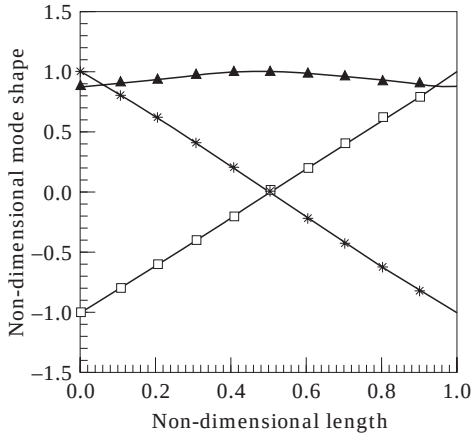

Figure 15. The fundamental shapes of free–free, doubly coupled beam: $\eta = 0$, $\eta_t = 0$, $f = 44{\cdot}58$ Hz, P_z excitation. –∗–, Bending; –□–, torsion; –▲–, warping.

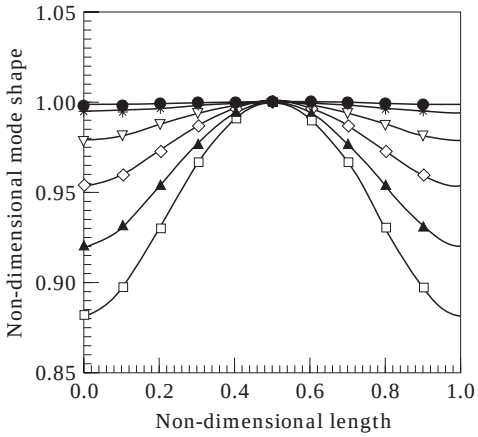

Figure 16. The fundamental warping shapes of free–free, doubly coupled beam: $\eta = 0$, $\eta_t = 0$, P_z excitation. –□–, $L = 1{\cdot}0$ m; –▲–, $L = 0{\cdot}8$ m; –◇–, $L = 0{\cdot}6$ m; –▽–, $L = 0{\cdot}4$ m; –∗–, $L = 0{\cdot}2$ m; –●–, $L = 0{\cdot}1$ m.

4. CONCLUSIONS

In this study, a new analytical approach is presented for the analysis of forced vibrations of open-section channels. Open-section channels, in which the centroid and the shear centre usually do not coincide, undergo vibrations which are inherently coupled. Hence any flexural vibration leads to the occurrence of torsional vibrations. The reverse of the statement also holds true. The analysis requires the simultaneous consideration of all the possible vibratory motions. The wave propagation approach is found to provide a good answer to this complicated problem and the method developed is based on it.

The current method analyzes the forced, coupled vibrations of open-section channels. The channels, taken as Euler–Bernoulli beams, have uniform cross-sections and, depending on their geometry, have either a single symmetry axis or no symmetry at all. These consecutively lead to double or triple coupling of vibrations. The excitation is assumed to be in the form of an harmonic point force.

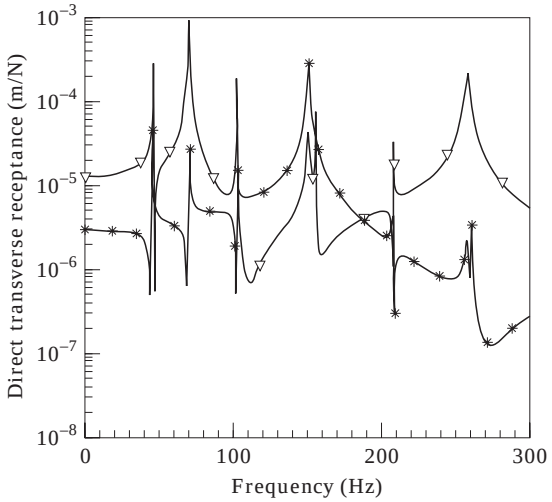

Figure 17. The direct frequency responses of triply coupled beam: $\eta = 0{\cdot}01$, $\eta_t = 0{\cdot}001$, $x_f = 0{\cdot}13579$ m, only mass coupling, no warping constraint. –∗–, w/P_z, –▽–, v/P_y.

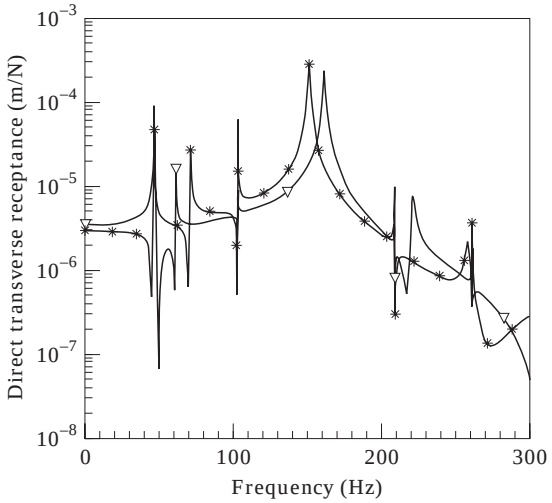

Figure 18. The direct transverse receptances (w/P_z) of triply coupled beam: $\eta = 0{\cdot}01$, $n_t = 0{\cdot}001$, $x_f = 0{\cdot}13579$ m, no warping constraint. $-*-$, Only mass coupling; $-\triangledown-$, mass and stiffness coupling.

In the study, the coupled wavenumbers were analyzed first. The detailed analysis showed the effects of mass and stiffness coupling and the warping constraint. Various frequency response curves of coupled vibrations were then presented for a variety of different classical end boundary conditions.

The method developed, although aimed at determining forced vibration characteristics, is also capable of determining the free vibration properties. This has been demonstrated by presenting various mode shape graphs.

The method can also be used in analyzing non-classical boundary conditions. Futhermore, the effects of multi-point and/or distributed loadings can also be determined through the proposed approach. This can be achieved simply by modifying the terms of the forcing vector without increasing the order of the relevant matrix equation. The method can also be used in the forced or free vibration analysis of uniform channels which are supported by any means at arbitrary locations along their length. On the other hand,

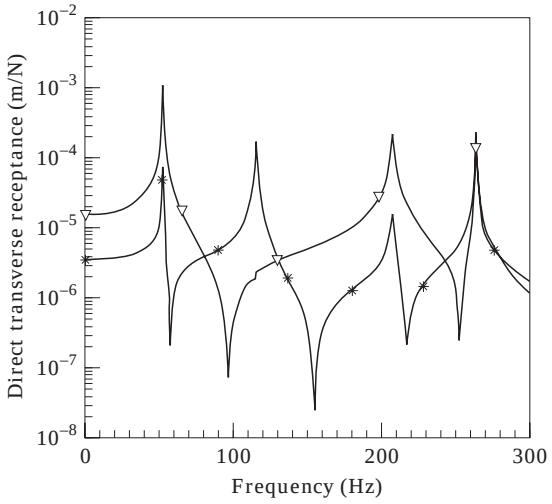

Figure 19. The direct transverse receptances of triply coupled beam: $\eta = 0{\cdot}01$, $\eta_t = 0{\cdot}001$, $x_f = 0{\cdot}13579$ m, mass and stiffness coupling, warping constraint included. $-*-$, w/P_z; $-\triangledown-$, v/P_y.

the present model does not account for the effects of the cross-sectional distortion of the channels, which may be important at very high frequencies.

Finally, it can be said that the proposed method, like the similar models of Bishop *et al*. [5], can serve as a convenient alternative to complicated techniques such as Vlasov theory and the finite element method in the analysis of coupled vibrations of uniform channels.

REFERENCES

1. J. M. Gere and Y. K. Lin 1958 *Journal of Applied Mechanics*, *Transactions of the American Society of Mechanical Engineers* **80**, 373–378. Coupled vibrations of thin-walled beams of open cross-section.
2. Y. K. Lin 1960 *Journal of Applied Mechanics*, *Transactions of the American Society of Mechanical Engineers* **82**, 739–740. Coupled vibrations of restrained thin-walled beams.
3. R. E. D. Bishop, W. G. Price and Zhang Xi-Cheng 1985 *Journal of Sound and Vibration* **99**, 155–167. A note on the dynamical behaviour of uniform beams having open channel section.
4. E. Dokumaci 1987 *Journal of Sound and Vibration* **119**, 443–449. An exact solution for coupled bending and torsion vibrations of uniform beams having single cross-sectional symmetry.
5. R. E. D. Bishop, S. M. Cannon and S. Miao 1989 *Journal of Sound and Vibration* **131**, 457–464. On coupled bending and torsional vibration of uniform beams.
6. L. Cremer and M. Heckl 1988 *Structure-borne Sound*. Berlin: Springer-Verlag.
7. D. J. Mead and Y. Yaman 1990 *Journal of Sound and Vibration* **141**, 465–484. The harmonic response of uniform beams on multiple linear supports: a flexural wave analysis.
8. D. J. Mead and Y. Yaman 1991 *Journal of Sound and Vibration* **144**, 507–530. The response of infinite periodic beams to a point harmonic force: a flexural wave analysis.
9. S. Timoshenko, D. H. Young and W. Weaver, Jr. 1974 *Vibration Problems in Engineering*. New York: John Wiley.

APPENDIX A: MATRIX EQUATIONS FOR CLAMPED AND FREE ENDS

A.1. WARPING CONSTRAINT EXCLUDED

A.1.1. *Clamped ends*

Assume that both of the ends of the channel are clamped. Then the required boundary conditions are

$$w(0) = w(L) = w'(0) = w'(L) = \phi(0) = \phi(L) = 0. \tag{A1}$$

When the $w(x)$ and $\phi(x)$ expressions given by equations (12) are substituted into equations (A1) the following matrix equation can be obtained:

$$\begin{bmatrix} 1 & 1 & 1 & 1 & 1 & 1 \\ k_1 & -k_1 & k_2 & -k_2 & k_3 & -k_3 \\ \Psi_1 & \Psi_1 & \Psi_2 & \Psi_2 & \Psi_3 & \Psi_3 \\ \Psi_1 e_1 & \Psi_1 e_{-1} & \Psi_2 e_2 & \Psi_2 e_{-2} & \Psi_3 e_3 & \Psi_3 e_{-3} \\ k_1 e_1 & -k_1 e_{-1} & k_2 e_2 & -k_2 e_{-2} & k_3 e_3 & -k_3 e_{-3} \\ e_1 & e_{-1} & e_2 & e_{-2} & e_3 & e_{-3} \end{bmatrix} \begin{Bmatrix} A_1 \\ A_2 \\ A_3 \\ A_4 \\ A_5 \\ A_6 \end{Bmatrix} = - \begin{Bmatrix} \sum_{n=1}^{3} a_n \, e^{-k_n x_f} \\ \sum_{n=1}^{3} k_n a_n \, e^{-k_n x_f} \\ \sum_{n=1}^{3} \Psi_n a_n \, e^{-k_n x_f} \\ \sum_{n=1}^{3} \Psi_n a_n \, e^{-k_n (L - x_f)} \\ \sum_{n=1}^{3} -k_n a_n \, e^{-k_n (L - x_f)} \\ \sum_{n=1}^{3} a_n \, e^{-k_n (L - x_f)} \end{Bmatrix}. \tag{A2}$$

Here k_n, Ψ_n and e_n are defined in section 2.2.

A.1.2. *Free ends*

If both ends are free, the required boundary conditions are

$$w''(0) = w''(L) = w'''(0) = w'''(L) = \phi'(0) = \phi'(L) = 0. \tag{A3}$$

The consideration of equations (A3), together with equations (12), leads to the following matrix equation:

$$\begin{bmatrix} k_1^2 & k_1^2 & k_2^2 & k_2^2 & k_3^2 & k_3^2 \\ k_1^3 & -k_1^3 & k_2^3 & -k_2^3 & k_3^3 & -k_3^3 \\ k_1\Psi_1 & -k_1\Psi_1 & k_2\Psi_2 & -k_2\Psi_2 & k_3\Psi_3 & -k_3\Psi_3 \\ k_1\Psi_1 e_1 & -k_1\Psi_1 e_{-1} & k_2\Psi_2 e_2 & -k_2\Psi_2 e_{-2} & k_3\Psi_3 e_3 & -k_3\Psi e_{-3} \\ k_1^3 e_1 & -k_1^3 e_{-1} & k_2^3 e_2 & -k_2^3 e_{-2} & k_3^3 e_3 & -k_3^3 e_{-3} \\ k_1^2 e_1 & k_1^2 e_{-1} & k_2^2 e_2 & k_2^2 e_{-2} & k_3^2 e_3 & k_3^2 e_{-3} \end{bmatrix} \begin{Bmatrix} A_1 \\ A_2 \\ A_3 \\ A_4 \\ A_5 \\ A_6 \end{Bmatrix} = - \begin{Bmatrix} \sum_{n=1}^{3} k_n^2 a_n e^{-k_n x_f} \\ \sum_{n=1}^{3} k_n^3 a_n e^{-k_n x_f} \\ \sum_{n=1}^{3} k_n \Psi_n a_n e^{-k_n x_f} \\ \sum_{n=1}^{3} -k_n \Psi_n a_n e^{-k_n (L - x_f)} \\ \sum_{n=1}^{3} -k_n^3 a_n e^{-k_n (L - x_f)} \\ \sum_{n=1}^{3} k_n^2 a_n e^{-k_n (L - x_f)} \end{Bmatrix}. \tag{A4}$$

A.2. WARPING CONSTRAINT INCLUDED

A.2.1. *Clamped ends*

Suppose that the ends are clamped. Then, one must satisfy the following boundary conditions:

$$w(0) = w(L) = w'(0) = w'(L) = \phi(0) = \phi(L) = \phi'(0) = \phi'(L) = 0. \tag{A5}$$

Substitution of $w(x)$ and $\phi(x)$ given by equations (12) into equations (A5) gives the following matrix equation:

Equation (A6) *overleaf*

$$
\begin{array}{r}
w(0):\\ w'(0):\\ \phi(0):\\ \phi'(0):\\ \phi'(L):\\ \phi(L):\\ w'(L):\\ w(L):
\end{array}
\begin{bmatrix}
1 & 1 & 1 & 1 & 1 & 1 & 1 & 1\\
k_1 & -k_1 & k_2 & -k_2 & k_3 & -k_3 & k_4 & -k_4\\
\Psi_1 & \Psi_1 & \Psi_2 & \Psi_2 & \Psi_3 & \Psi_3 & \Psi_4 & \Psi_4\\
k_1\Psi_1 & -k_1\Psi_1 & k_2\Psi_2 & -k_2\Psi_2 & k_3\Psi_3 & -k_3\Psi_3 & k_4\Psi_4 & -k_4\Psi_4\\
k_1\Psi_1 e_1 & -k_1\Psi_1 e_{-1} & k_2\Psi_2 e_2 & -k_2\Psi_2 e_{-2} & k_3\Psi_3 e_3 & -k_3\Psi_3 e_{-3} & k_4\Psi_4 e_4 & -k_4\Psi_4 e_{-4}\\
\Psi_1 e_1 & \Psi_1 e_{-1} & \Psi_2 e_2 & \Psi_2 e_{-2} & \Psi_3 e_3 & \Psi_3 e_{-3} & \Psi_4 e_4 & \Psi_4 e_{-4}\\
k_1 e_1 & -k_1 e_{-1} & k_2 e_2 & -k_2 e_{-2} & k_3 e_3 & -k_3 e_{-3} & k_4 e_4 & -k_4 e_{-4}\\
e_1 & e_{-1} & e_2 & e_{-2} & e_3 & e_{-3} & e_4 & e_{-4}
\end{bmatrix}
\begin{Bmatrix} A_1\\ A_2\\ A_3\\ A_4\\ A_5\\ A_6\\ A_7\\ A_8 \end{Bmatrix}
= -
\begin{Bmatrix}
\sum_{n=1}^{4} a_n e^{-k_n x_f}\\
\sum_{n=1}^{4} k_n a_n e^{-k_n x_f}\\
\sum_{n=1}^{4} \Psi_n a_n e^{-k_n x_f}\\
\sum_{n=1}^{4} k_n \Psi_n a_n e^{-k_n x_f}\\
\sum_{n=1}^{4} -k_n \Psi_n a_n e^{-k_n (L-x_f)}\\
\sum_{n=1}^{4} \Psi_n a_n e^{-k_n (L-x_f)}\\
\sum_{n=1}^{4} -k_n a_n e^{-k_n (L-x_f)}\\
\sum_{n=1}^{4} a_n e^{-k_n (L-x_f)}
\end{Bmatrix}. \tag{A6}
$$

A.2.2. *Free ends*

If both ends are free, the boundary conditions to be satisfied become

$$w''(0) = w''(L) = w'''(0) = w'''(L) = T(0) = T(L) = \phi''(0) = \phi''(L) = 0. \tag{A7}$$

Utilization of equations (10), (12) and (A7) yields the following matrix equation, in which $\beta_n = -k_n\,(GJ - k_n^2\,E\Gamma_0)\Psi_n$:

$$
\begin{array}{c}
\\
w''(0): \\
w'''(0): \\
T(0): \\
\phi''(0): \\
\phi''(L): \\
T(L): \\
w'''(L): \\
w''(L):
\end{array}
\begin{bmatrix}
k_1^2 & k_1^2 & k_2^2 & k_2^2 & k_3^2 & k_3^2 & k_4^2 & k_4^2 \\
k_1^3 & -k_1^3 & k_2^3 & -k_2^3 & k_3^3 & -k_3^3 & k_4^3 & -k_4^3 \\
k_1\beta_1 & -k_1\beta_1 & k_2\beta_2 & -k_2\beta_2 & k_3\beta_3 & -k_3\beta_3 & k_4\beta_4 & -k_4\beta_4 \\
k_1^2\Psi_1 & k_1^2\Psi_1 & k_2^2\Psi_2 & k_2^2\Psi_2 & k_3^2\Psi_3 & k_3^2\Psi_3 & k_4^2\Psi_4 & k_4^2\Psi_4 \\
k_1^2\Psi_1 e_1 & k_1^2\Psi_1 e_{-1} & k_2^2\Psi_2 e_2 & k_2^2\Psi_2 e_{-2} & k_3^2\Psi_3 e_3 & k_3^2\Psi_3 e_{-3} & k_4^2\Psi_4 e_4 & k_4^2\Psi_4 e_{-4} \\
k_1\beta_1 e_1 & -k_1\beta_1 e_{-1} & k_2\beta_2 e_2 & -k_2\beta_2 e_{-2} & k_3\beta_3 e_3 & -k_3\beta_3 e_{-3} & k_4\beta_4 e_4 & -k_4\beta_4 e_{-4} \\
k_1^3 e_1 & -k_1^3 e_{-1} & k_2^3 e_2 & -k_2^3 e_{-2} & k_3^3 e_3 & -k_3^3 e_{-3} & k_4^3 e_4 & -k_4^3 e_{-4} \\
k_1^2 e_1 & k_1^2 e_{-1} & k_2^2 e_2 & k_2^2 e_{-2} & k_3^2 e_3 & k_3^2 e_{-3} & k_4^2 e_4 & k_4^2 e_{-4}
\end{bmatrix}
\begin{Bmatrix} A_1 \\ A_2 \\ A_3 \\ A_4 \\ A_5 \\ A_6 \\ A_7 \\ A_8 \end{Bmatrix}
=
-\begin{Bmatrix}
\sum_{n=1}^{4} k_n^2 a_n \mathrm{e}^{-k_n x_f} \\
\sum_{n=1}^{4} k_n^3 a_n \mathrm{e}^{-k_n x_f} \\
\sum_{n=1}^{4} k_n \Psi_n a_n \mathrm{e}^{-k_n x_f} \\
\sum_{n=1}^{4} k_n^2 \Psi_n a_n \mathrm{e}^{-k_n x_f} \\
\sum_{n=1}^{4} k_n^2 \Psi_n a_n \mathrm{e}^{-k_n (L - x_f)} \\
\sum_{n=1}^{4} -k_n \Psi_n a_n \mathrm{e}^{-k_n (L - x_f)} \\
\sum_{n=1}^{4} -k_n^3 a_n \mathrm{e}^{-k_n (L - x_f)} \\
\sum_{n=1}^{4} k_n^2 a_n \mathrm{e}^{-k_n (L - x_f)}
\end{Bmatrix}. \tag{A8}
$$

APPENDIX B: NOMENCLATURE

a_n	nth transverse displacement coefficient in the z direction
b_n	nth transverse displacement coefficient in the y direction
c_n	nth torsional displacement coefficient
c_y	eccentricity in the y direction
c_z	eccentricity in the z direction
h	web height of the channel
k_n	nth wavenumber
m	mass per unit length of channel
t	time
u	warping displacement
v	transverse displacement in the y direction
x, y, z	spatial variables; co-ordinate system
w	transverse displacement in the z direction
A	constant channel cross-sectional area
C	centroid of channel
E	Young's modulus
G	shear modulus
I_0	polar second moment of area about shear centre
I_v	second moment of area about the v-axis
$I_{v\xi}$	product moment of area about the v- and ξ-axes
I_ξ	second moment of area about the ξ-axis
J	torsion constant
L	length of channel
O	shear centre of channel
P_y	transverse load in the y direction
P_z	transverse load in the z direction
T	resulting torque about shear centre
v, ξ	centroidal axes
ϕ	torsional displacement
ρ	material density
ω	angular frequency
η	flexural damping coefficient
η_t	torsional damping coefficient
Γ_0	warping constant about shear centre
i	$=\sqrt{-1}$
$'$	$=\partial/\partial x$
$''$	$=\partial^2/\partial x^2$
$'''$	$=\partial^3/\partial x^3$
$\|\|$	absolute value

Dummy variables confined to certain sections are clearly defined wherever applicable.